

FINAL-FOCUS SUPERCONDUCTING MAGNETS FOR SUPERKEKB*

N. Ohuchi[†], Y. Arimoto, K. Aoki, M. Kawai, T. Kawamoto, H. Koiso, Y. Kondo, M. Masuzawa, A. Morita, S. Nakamura, Y. Ohnishi, T. Oki, Y. Ohsawa, H. Sugimoto, K. Tsuchiya, R. Ueki, X. Wang, H. Yamaoka, Z. Zong, KEK, Tsukuba, Japan
 P. Wanderer, B. Parker, M. Anerella, J. Escallier, A. Marone, A. Jain, BNL, Upton, USA
 G. Velev, J. DiMarco, J. Nogiec, M. Tartaglia, T. Gardner, FNAL, Batavia, USA
 T. Kim, Mitsubishi Electric Corporation, Kobe, Japan

Abstract

SuperKEKB is now being operated with the final focus system as the phase-2 commissioning from March 16th, 2018. The final focus system is the key device to attain the target luminosity of $8 \times 10^{35} \text{ cm}^{-2} \text{ s}^{-1}$. Designing the system had started from 2009, and the construction was completed in March 2017. The final focus system consists of 55 superconducting magnets, and they were assembled carefully in two cryostats under the very tight space constraints. This paper describes the design configuration of the system, and reports the results of the commissioning on the beam lines in the SuperKEKB interaction region.

INTRODUCTION

SuperKEKB [1, 2] is the upgraded accelerator of KEKB [3], and the special feature of SuperKEKB is in the point where the nano-beam scheme [4] was applied to the colliding method. The beams of 7 GeV electrons as the high energy ring (HER) and 4 GeV positrons as the high energy ring (LER) collide at the interaction point (IP) with the large crossing angle of 83 mrad. The target luminosity was designed to be $8 \times 10^{35} \text{ cm}^{-2} \text{ s}^{-1}$ and two beams are squeezed to about 50 nm at IP in the design.

The phase-1 commissioning of SuperKEKB without the final focus system [5] was successfully conducted from February 1st, 2016 to June 28th, 2016. After this beam operation, the installation of the final focus system into the interaction region (IR) was begun from August 2016, and the construction was completed in the end of March, 2017. The cooling and excitation tests of the superconducting (SC) magnets and the magnetic field measurements on the beam lines were performed from May, 2017 to August 2017. In this paper, the configuration of the final focus system of SuperKEKB is described, and the construction of the magnets and the field measurement results on the beam lines are reported.

SUPERCONDUCTING MAGNET SYSTEM

System Layout of the Final Focus System

The final focus system consists of the 55 SC magnets. The 25 and 30 magnets were assembled in the left and right cryostats, QCSL and QCSR, respectively. Figure 1 shows the system layout of the SC magnets in the two cryostats. They are classified into three types of the SC magnets:

main quadrupole magnets [6-8], corrector magnets [9, 10] and compensation solenoid magnets, ESL [11] and ESR1/2/3.

Figure 2 shows the horizontal cross section of IR. Two cryostats are completely installed inside the Belle-II detector [12]. The SC solenoid of the Belle-II detector generates the solenoid magnetic field at 1.5 T at the center of the detector, and therefore the 55 SC magnets are designed to be operated under this solenoid field.

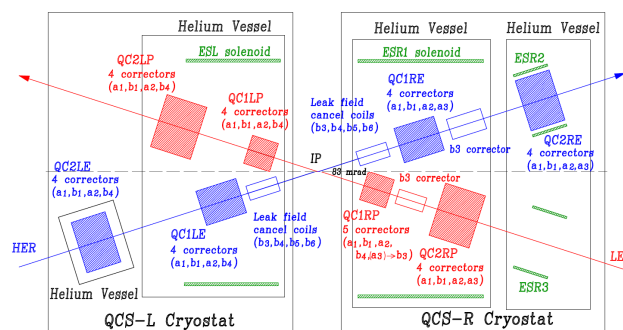


Figure 1: Layout of superconducting magnets in IR.

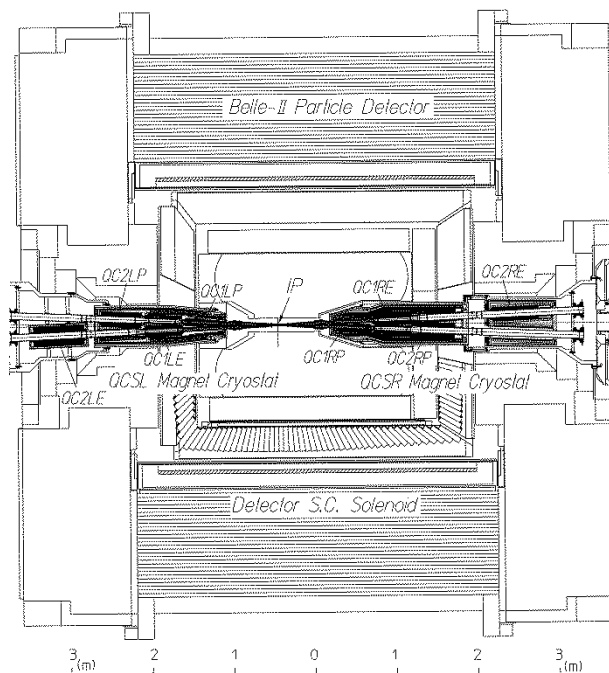


Figure 2: Horizontal cross section of the magnet-cryostats and the Belle II detector.

* Work supported by US-Japan Science and Technology Cooperation Program in High Energy Physics

[†] Norihito.ohuchi@kek.jp

Content from this work may be used under the terms of the CC BY 3.0 licence (© 2018). Any distribution of this work must maintain attribution to the author(s), title of the work, publisher, and DOI.

Final Focus Quadrupole Magnets

Focusing and defocusing beams in IR are performed with the quadrupole doublets on each beam line. Along the LER and HER beam lines, the QC1RP/LP, QC2RP/LP, QC1RE/LE and QC2RE/LE magnets are positioned as shown in Figs. 1 and 2. The design parameters of the magnets are listed in Table 1. QC1RP/LP locate at the positions of +/-935 mm from IP, respectively, and these magnets have not the magnetic yokes. The other magnets have the magnetic yokes. The quadrupole magnets for LER have the roll angles with respect to the horizontal plane, and the magnetic centers are shifted in a vertical direction. The quadrupole magnets for HER are designed to be aligned with the roll angle of 0 mrad and with the horizontal shifts of the magnetic centers.

Table 1: Design Parameters of Quadrupole Field

Mag.	Z	GL	θ	Δx	Δy
QC2RE	2925	13.04	0	-0.7	0.0
QC2RP	1925	11.54	-2.114	0.0	-1.0
QC1RE	1410	25.39	0	-0.7	0.0
QC1RP	935	22.96	7.204	0.0	-1.0
QC1LP	-935	22.96	-13.65	0.0	-1.5
QC1LE	-1410	26.94	0	+0.7	0.0
QC2LP	-1925	11.48	-3.725	0.0	-1.5
QC2LE	-2700	15.27	0	+0.7	0.0

Z (mm): longitudinal field center position from IP, GL (T): integral field gradient, θ (mrad): roll angle of the field mid-plane, Δy (mm): vertical shift of the field center from the horizontal plane including IP, and Δx (mm): horizontal field center shift from the design beam line through IP.

Corrector Magnets

The 43 SC corrector magnets were assembled in the system. Because of the space constraint in the cryostats, the corrector magnets were manufactured by the direct winding method by BNL [13] under the research collaboration of the US-Japan Science and Technology Cooperation Program in High Energy Physics.

In Table 2, the specific field strengths of the corrector magnets for the beam operation are summarized. The a_1 , b_1 and a_2 corrector magnets are used as the magnetic alignment devices of the magnetic field centers and the mid-plane angles. These corrector magnets are placed inside of the quadrupole magnet bores in the multi-layered structure. The a_3 and b_3 magnets are used for the correction of the sextupole field induced by the assembly errors of the quadrupole magnets. The b_4 magnets are assembled for improving the dynamic apertures.

Since QC1RP/LP have not the magnetic yokes, the leak field from the magnets to the HER beam line is over 0.1 T, and it contains all multipole field components. The field profile along the beam line at the nominal current of QC1LP is shown in Fig. 3. In the figure, Z corresponds to the position from IP. The B_1 and B_2 field components are included in the beam optics design, and the B_3 , B_4 , B_5 and B_6 field components are cancelled by the special shaped corrector magnets [10].

Table 2: Field Strength of Corrector from Optics

Magnet	a_1 Tm	b_1 Tm	a_2 T	a_3 T/m	b_3 T/m	b_4 T/m ²
QC2RE	0.015	0.015	0.37	1.05	NA	NA
QC2RP	0.03	0.03	0.31	0.91	NA	NA
QC1-2RE	NA	NA	NA	NA	18.2	NA
QC1-2RP	NA	NA	NA	NA	11.5	NA
QC1RE	0.027	0.046	0.75	4.55	NA	NA
QC1RP	0.016	0.016	0.64	5.1	NA	60
QC1LP	0.016	0.016	0.64	NA	NA	60
QC1LE	0.027	0.046	0.75	NA	NA	60
QC2LP	0.03	0.03	0.31	NA	NA	60
QC2LE	0.015	0.015	0.37	NA	NA	60

QC1-2RE and QC1-2RP correspond the areas between QC1 and QC2 for HER and LER beam lines in QCSR, respectively.

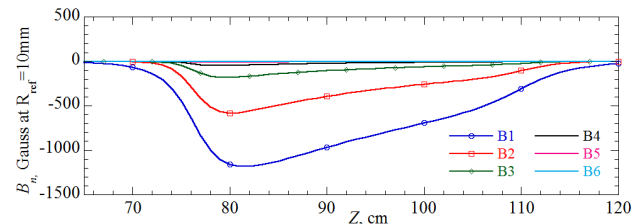


Figure 3: Leak field profiles along the HER beam line.

Compensation Solenoid Magnets

Figure 4 shows the solenoid field profile (red line) only by the Belle-II solenoid magnet and the combined field profile (black line) with ESL and ESR1/2/3 with the locations of the quadrupole magnets. As shown in Fig. 5, Belle-II solenoid generates the magnetic field of 1.5 T at the center of the detector, and the field is cancelled by the reverse solenoid fields in the areas of QC1LP and QC1RP. Since QC1RE/LE and QC2RP/LP have the Permendur yokes and the counter beam lines are covered by the magnetic shields, the combined fields on the beam lines are designed to be less than 0.01 T. The residual solenoid fields on the beam lines are negligible for the beam operation. Between QC2RP and QC2RE, the Belle-II fringe field is in the range of 0.6 T because of no magnetic shields. The fringe field is cancelled by ESR2 or ESR3 in the area of QC2RE.

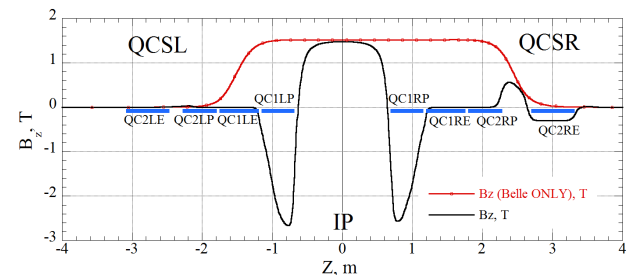


Figure 4: Solenoid field profiles along the beam lines.

CONSTRUCTION OF SC MAGNETS

SC Quadrupole Magnets (QC1, QC2)

The quadrupole magnets which locate at the symmetric positions with respect to IP, like QC1LP and QC1RP, have the same magnet cross section. For the four magnets in the same side to IP, the different cross sections were designed because of the different beam physical apertures. In Fig. 5, the four cross sections of the quadrupole magnets are shown. The SC quadrupole magnet consists

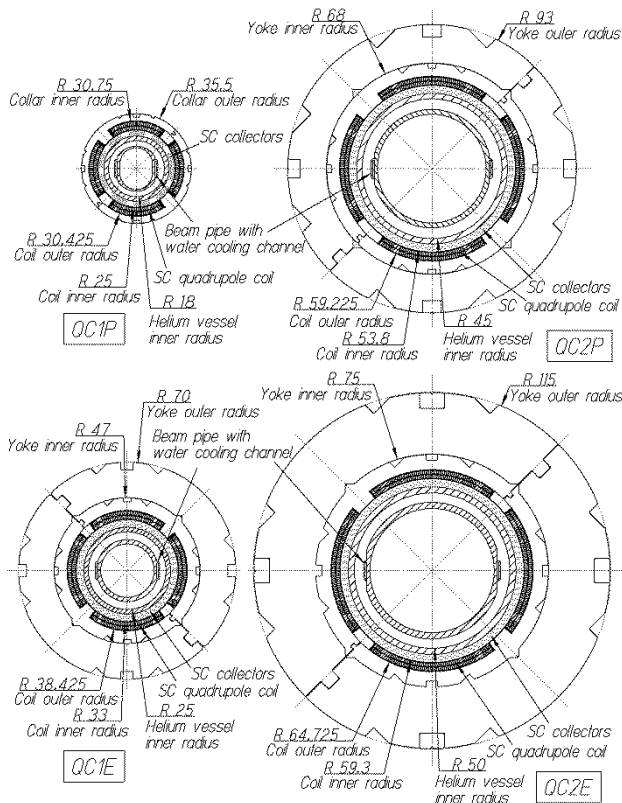


Figure 5: Cross section design of SC quadrupole magnets.

Table 3: Design Parameters for Quadrupole Magnets

Parameter	QC1P	QC1E	QC2P	QC2E
G_D , T/m	76.37	91.57	31.97	36.39
I_D , A	1,800	2,000	1,000	1,250
B_P , T	4.56	3.5	2.43	2.63
LR, %	72.3	73.4	44	39
R_C , mm	25.0	33.0	53.8	59.3
R_{Y_0} , mm	NA	70.0	93.0	115.0
L_{PM} , mm	409.3	455.4	495.5	618.9
L_{EM} , mm	333.6	373.1	409.9	537.0
Cable	NbTi	NbTi	NbTi	NbTi
θ_K , deg.	2.1	1.6	1.0	0.94

G_D : design field gradient at the magnet center, I_D : magnet design current, B_P : maximum field in the coil at I_D , LR: load line ratio to the critical point, R_C : SC coil inner radius, R_{Y_0} : yoke outer radius, L_{PM} : magnet physical length, L_{EM} : effective magnetic length, θ_K : key stone angle of the SC cable

of the two layer SC coils (double-pancake structure). For the coils, the Rutherford type NbTi cables were used. The cable consists of 10 strand wires of $\phi 0.5$ mm. In order to manufacture the coils precisely, the key-stone angles of the cables were specified for each magnet. In Table 3, the main parameters of the magnets are shown. The production of the SC coils for QCSL started from December 2012. In Figs. 6 and 7, the SC coils for QC1LP and the completed QC1LP are shown. The construction of all quadrupole magnets was completed in March 2014.



Figure 6: Four SC coils for QC1LP.



Figure 7: QC1LP with corrector magnets.

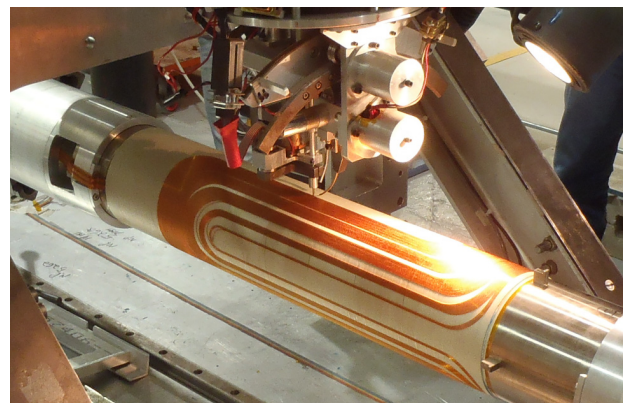


Figure 8: Winding process of corrector magnets in BNL.

SC Corrector Magnets

SC corrector magnets had been developed from 2011 in BNL, and 43 corrector magnets were completed in February 2015. The winding of the SC coil was performed by the computer controlled winding robot, and the SC wire of $\phi 0.35$ mm was directly stuck on the outer surface of the support bobbin as the helium inner vessel. After the production

Content from this work may be used under the terms of the CC BY 3.0 licence (© 2018). Any distribution of this work must maintain attribution to the author(s), title of the work, publisher, and DOI.

of the magnet, the field measurements at room temperature were performed in BNL. The excitation tests and the field measurements in liquid helium were performed in KEK after delivery to KEK. In Fig. 8, the winding process of the corrector magnet in BNL is shown.

Compensation Solenoids (ESL, ESR1/2/3)

The first function of the compensation solenoids is cancelling the integral Belle-II solenoid field from IP, and in addition, the combined filed profiles along the beam lines are optimized for minimizing the beam emittance. In order to produce the required field profile by the beam optics, ESL and ESR1 solenoids consist of the 12 and 15 small solenoids, respectively. In Fig. 9, ESR1 is shown. Inside the solenoid bore, QC1RP/RE and QC2RP were assembled. The magnet parameters are listed in Table 4.



Figure 9: ESR1 compensation solenoid.

Table 4: Design Parameters for Compensation Solenoids

	ESL	ESR1	ESR2/3
Integral field, Tm	2.31	3.69	0.17
I, A	390	450	151
Inductance, H	2.5	8.0	0.14
Max. field, T	3.4	3.2	0.48
Magnet length, mm	905	1575	720
LR, %	52	51	11

Assembly of SC Magnets Into The Cryostats

55 superconducting magnets were assembled into two cryostats. In the cryostat, the SC magnets were assembled in the front and rear helium vessels, and the helium vessels were aligned within +/-0.2 mm to the alignment targets on the outer surface of the cryostats. Figure 10 shows the front cold mass for QCSL. In the cold mass, 19 SC magnets were assembled. The assembly accuracy of the components to the design positions was within +/- 50 μ m.

The QCSL magnet cryostat was delivered to KEK at December 25th, 2015, and after performance tests in the experimental laboratory on the ground, the cryostat was installed into IR in August 2016. The QCSR magnet cryostat was delivered to KEK at February 13th, 2017, and it was installed to IR on the day. Figure 11 shows the two cryostats in IR. In the picture, the cryostat in the left hand side is the QCSR cryostat. The blue large device in the back is the Belle-II detector.

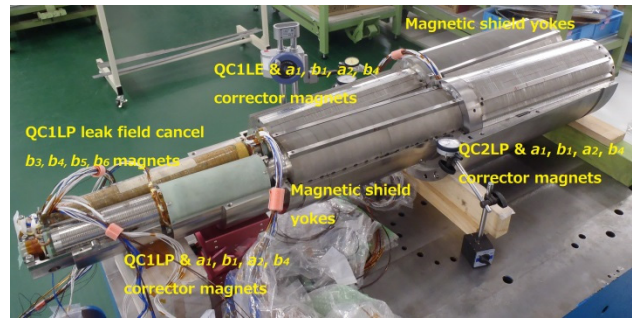


Figure 10: Assembled SC magnets in the front helium vessel of the QCSL cryostat.

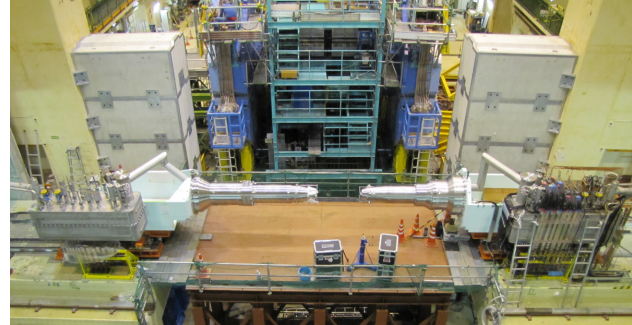


Figure 11: QCSL/R cryostats and Belle-II detector in IR.

COMMISSIONING OF SYSTEM

The commissioning of the system was performed after assembling cryostats into the Belle-II detector from May 2017 to August 2017. The magnet cryostats were cooled down to 4 K by the individual helium refrigerators. In the magnet performance tests, the excitation to the operation currents, the magnetic field measurements and the operation stability of the system including the cryogenic system and the power supplies were confirmed. As for the magnetic field performances of the SC magnets, three types of the probes were applied: the single stretched wire (SSW), the harmonic coils and the Hall sensor. In the following section, the magnetic field measurement results are reported.

Table 5: Errors of Quadrupole Center and Angle by SSW

Magnet	Δx , mm	Δy , mm	θ , mrad
QC2RP	0.49	0.04	-3.84
QC1RP	0.68	-0.30	9.22
QC1LP	0.01	-0.21	-15.32
QC2LP	-0.34	-0.69	-7.77
QC2RE	0.08	-0.58	-0.73
QC1RE	0.25	-0.37	-0.14
QC1LE	-0.21	-0.29	-1.60
QC2LE	0.13	-0.54	-1.54

SSW Measurements

The SSW system for the final focus system of SuperKEKB was developed by FNAL under the US-Japan

Science and Technology Cooperation Program in High Energy Physics. The SSW system measured directly the magnetic centers and the field mid-plane angles of the quadrupole magnets. During the measurements, the Belle-II solenoid was excited to 1.5 T. The BeCu wire of ϕ 0.1 mm went through two cryostat bores on each beam line, and the wire was aligned with respect to the design beam line at the positions in the backward of both cryostats. The measured results are listed in Table 5. All alignment errors of the magnetic centers and the field angles are able to be corrected with the corrector magnets.

Field Quality Measurements by Harmonic Coils

The error field components of the SC magnets were measured with 3 sets of the harmonic coils. In order to have a resolution at the level of 1×10^{-5} with respect to the quadrupole field component, the harmonic coil radii were designed to be 12 mm, 25mm and 33 mm for QC1P/E, QC2P and QC2E, respectively, and the analog and digital bucking method [14] of the quadrupole field were applied. The measured higher order field components are listed in Tables 6 and 7. The multi-pole field components are expressed as the ratio with respect to the quadrupole field components as 10,000 at the reference radius of each magnet. The error field components of the 8 quadrupole magnets are well controlled during the production, and the sextupole field components are within the tolerable level to have a sufficient beam life time.

Table 6: Multipole Components of KER Quadrupoles

<i>n</i>	QC1LP R=10 mm		QC1RP R=10 mm		QC2LP R=30 mm		QC2RP R=30 mm	
	<i>a_n</i>	<i>b_n</i>	<i>a_n</i>	<i>b_n</i>	<i>a_n</i>	<i>b_n</i>	<i>a_n</i>	<i>b_n</i>
3	-0.1	1.7	0.7	-0.9	1.0	-2.6	-2.6	0.1
4	0.5	0.0	-0.9	-0.7	-0.2	0.2	1.5	0.2
5	0.0	-0.4	-0.4	0.4	-0.9	-0.3	0.2	0.1
6	-0.3	-0.1	0.4	-0.1	-0.3	3.6	-0.6	4.7
7	0.0	-0.1	0.0	-0.1	0.0	-0.0	0.2	-0.0
8	0.1	-0.0	-0.0	-0.0	-0.1	-0.0	0.1	-0.1
9	0.1	-0.1	-0.0	0.1	0.5	-0.0	0.1	0.2
10	-0.0	-0.2	0.0	-0.2	-0.2	-0.9	-0.3	-1.8

Table 7: Multipole Components for HER Quadrupoles

<i>n</i>	QC1LE R=15 mm		QC1RE R=15 mm		QC2LE R=35 mm		QC2RE R=35 mm	
	<i>a_n</i>	<i>b_n</i>	<i>a_n</i>	<i>b_n</i>	<i>a_n</i>	<i>b_n</i>	<i>a_n</i>	<i>b_n</i>
3	-0.6	0.7	1.0	-0.5	1.4	1.2	4.8	2.9
4	0.2	-0.2	-0.1	-0.2	1.9	0.3	-0.6	-0.0
5	-0.2	-0.3	0.0	0.0	0.6	-0.2	-0.4	0.1
6	0.0	1.0	-0.1	0.9	-0.2	4.7	0.2	2.0
7	0.0	0.1	0.1	-0.0	0.0	-0.0	0.1	-0.1
8	-0.1	-0.1	0.0	-0.0	0.2	-0.1	-0.1	-0.1
9	-0.2	0.6	0.1	0.2	0.2	0.2	0.0	0.2
10	-0.1	-0.1	-0.0	-0.6	-0.1	-2.2	-0.1	-1.8

Solenoid Field Profile Measurement by Hall Probe

The solenoid field profiles along the beam lines were measured with the commercial 3-axis Hall probe. From the measurement, ESL was found out to compensate excessively the integral solenoid field by Belle-II solenoid. The transport current of the ESL was tuned from 404 A to 390 A. The analysis of the solenoid field is going on with the measured data and the 3D magnetic field calculation. The calibration of the Hall probe is scheduled for comparison with the calculation data.

CONCLUSION

The construction of the SuperKEKB final focus system was completed. Commissioning of the system was carried out from May-August 2017. The magnetic performances of 55 superconducting magnets were confirmed with three types of the measuring devices.

The Phase-2 commissioning of SuperKEKB is now going on, and the measured parameters of the magnets have been included in the beam operation. These magnet parameters will be checked from the beam diagnosis to attain the luminosity of $8 \times 10^{35} \text{ cm}^{-2} \text{ s}^{-1}$.

ACKNOWLEDGEMENT

The authors would like to thank Kazuyuki Aoki, Manabu Tanaka and Tomonari Endoh for their excellent technical supports in order to design, construct and operate the system.

REFERENCES

- [1] H. Koiso *et al.*, in *Proc. IPAC'11*, pp. 1931-1935.
- [2] Y. Ohnishi, presented at *IPAC'18* Vancouver, Canada, Apr-May 2018, paper MOXGB1, this conference.
- [3] S. Kurokawa *et al.*, NIM PR-A 499, pp. 1-233, 2003.
- [4] P. Raimondi, 2nd SuperB Meeting, Frascati, 2006.
- [5] N. Ohuchi *et al.*, in *Proc. of NA-PAC'13*, Pasadena CA, USA, Sept. 2013, pp. 759-761.
- [6] N. Ohuchi *et al.*, *IEEE Transactions on Appl. Supercond.*, Vol. 25, No. 3, June 2015, 4001202.
- [7] N. Ohuchi *et al.*, in *Proc. of IPAC'16*, Busan, Korea, May 2016, pp. 1174-1176.
- [8] Y. Arimoto *et al.*, in *Proc. of IPAC'16*, Busan, Korea, May 2016, pp. 3771-3773.
- [9] B. Parker *et al.*, in *Proc. of NA-PAC'13*, Pasadena CA, USA, Sept. 2013, pp. 1241-1243.
- [10] B. Parker *et al.*, in *Proc. of IPAC'16*, Busan, Korea, May 2016, pp. 1193-1195.
- [11] X. Wang *et al.*, *IEEE Trans. Appl. Supercond.*, 2016 Vol. 26, No. 4, 4102205.
- [12] Belle II Technical Design Report; <https://arxiv.org/abs/1011.0352>
- [13] B. Parker *et al.*, *IEEE Trans. Appl. Supercond.*, 2012 Vol. 22, No. 3, 4101604.
- [14] A. Jain, CERN 98-05, pp.175-217, 1998.